A New Programmable Load for Noise Parameter Determination

Björn M. Albinsson, *Student Member, IEEE*, Henglo Guo, Martin Schöön, *Student Member, IEEE*, and Hans-Olof Vickes, *Student Member, IEEE*

Abstract—**A new computer-controlled programmable load is presented. The load consists of a cascade of p-i-n diodes bonded to each other. The capacitance of the reverse-biased p-i-n diode, together with the interconnecting bonding wires, forms an artificial transmission line. A complete phase coverage in the Smith chart is obtained by forward-biasing any diode pair, using only two current generators and two multiplexers. The amplitude coverage will depend on the diode spacing. The load may be set to any reflection coefficient within its coverage area. Synthesis formulas for the determination of the current driver settings have been derived. A calibration procedure determining the unknown synthesis parameters from input port measurements only is presented. Only the p-i-n diode parameters are characterized separately. The programmable load has been built and tested. Measurements verify the principle and show good agreement with computer simulations. The load has been developed for noise parameter determination. Other applications for variable impedance measurements are circuit or device optimization of gain and output power performance.**

I. Introduction

An experimental search technique for noise parameter extraction of a linear two-port device was proposed by an IRE subcommittee in 1960 [1]. The device noise parameters ($F_{\min}, R_n, G_{\text{opt}}, B_{\text{opt}}$) were determined by curve fitting to experimental data. It was recognized by the committee that the method had practical limitations when the minima of the F-versus B_s and F versus G_s curves were shallow. $Y_s = G_s + jB_s$ is the source admittance. The method is furthermore tedious and not suited to computer implementation. A computerized approach to overcome these difficulties was proposed by Lane in 1969 [2]. The noise figure, $F(Y_s)$, of the device was measured for at least four different settings of the source admittance Y_s. By using a linearization of the noise figure equation and applying least square fitting, the noise parameters were extracted from the measured data. To automate the measurements, the noise figure meter and the source admittance must be controllable by a computer.

The programmable load is usually realized as either a one-port or a two-port. An isolator has to be included to reduce the input reflection coefficient of the two-port tuner. A change in the reflection coefficient for the noise source between ON and OFF states will otherwise cause the DUT to change noise figure and available gain [3]. The noise power input to the DUT will vary, as the two-port will reflect the noise differently depending on its setting. This will change the total loss and has to be monitored. A common configuration for the two-port programmable load is the motor-driven double stub tuner [4]. The one-port measurement setup requires an additional component to inject the noise, which is usually a coupler. The number of components is the same as for the two-port setup. The coupler buffers the noise source and no isolator is necessary. The noise power presented to the DUT will be stable but has been decreased by the coupling. This loss must be taken into account when the noise source ENR is chosen. Because of the coupler we obtain a decreased $|\Gamma|$. This is not necessarily a disadvantage when the DUT is a conditionally stable active device. A one-port programmable load generating discrete impedances in the Smith chart has been reported by Leake [5]. The load will generate discrete impedances in a number depending on the number of diode state combinations. However, discrete impedances are frequency dependent and it is found that they will not be well distributed in the Smith chart as frequency varies.

This paper presents an alternative approach where the programmable load may be set continuously within its coverage area. A desired pattern can therefore be achieved at any frequency, thereby offering a greater degree of flexibility and consistency. A number of p-i-n diodes are bonded to each other, forming an artificial transmission line [7]. By using only two continuous drivers multiplexed to any diode pair, the load may be set to any reflection coefficient within the coverage area. The coverage area is determined by the diode spacing and the loss of the artificial line.

II. Theory of Operation

A. Basic Configuration

A model of a p-i-n diode is shown in Fig. 1. As an ideal component the p-i-n diode may be represented by a variable resistance covering values from zero to infinity. The basic configuration of the programmable load realized by ideal p-i-n diodes is shown in Fig. 2. When the p-i-n diodes are reversed biased, the transmission will be complete and all of the power will be dissipated in the terminating resistance r_L. If the first diode is fully forward biased, the reflection coefficient will have a phase of 180°. If the diodes now are fully forward biased one by one, the phase of the reflection coefficient will decrease in steps of θ [7]. In this paper we control the bias current continuously to obtain any desired

Manuscript received January 3, 1990; revised September 20, 1990.

B. M. Albinsson was with the Division of Network Theory, Chalmers University of Technology, Gothenburg, Sweden. He is now with the Department of Applied Electron Physics, Chalmers University of Technology, S-412 96 Gothenburg, Sweden.

H. Guo was with the Department of Radio and Space Science, Chalmers University of Technology, Gothenburg, Sweden. He is now with Technophone AB, Södertälje, Sweden.

M. Schöön is with the Division of Network Theory, Chalmers University of Technology, S-412 96 Gothenburg, Sweden.

H.-O. Vickes was with the Division of Network Theory, Chalmers University of Technology, Gothenburg, Sweden. He is now with the Aerospace Division, Ericsson Radar Electronics, Mölndal, Sweden.

IEEE Log Number 9041094.

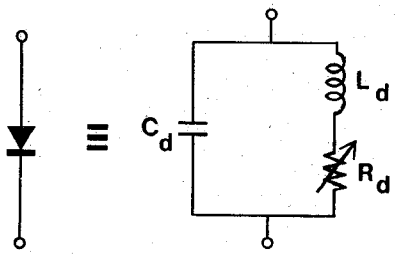

Fig. 1. Model of p-i-n diode.

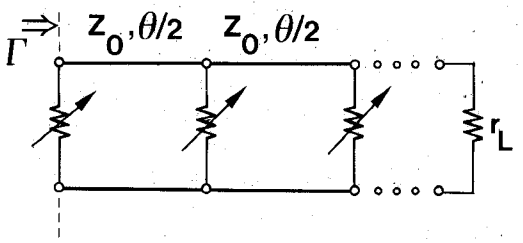

Fig. 2. Basic configuration with ideal components.

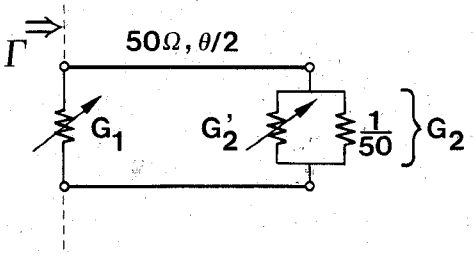

Fig. 3. Ideal diodes separated by a transmission line with length $\theta/2$.

phase shift rather than using a finite number of discrete states. In this way we can obtain any reflection coefficient inside the coverage area.

Let us study the input reflection coefficient variation in the Smith chart in order to find the coverage area. Consider two ideal p-i-n diodes separated by a transmission line (Fig. 3). When the transmission line is short-circuited on the right-hand side, the input admittance of the circuit is given by

$$y_d = G_1 - \frac{j}{50}\cot\frac{\theta}{2}. \tag{1}$$

By now letting G_1 vary from zero to infinity, the corresponding reflection coefficient, Γ_d, will move along a constant-susceptance arc (Fig. 4). For each setting of G_2, it is possible to traverse all constant-susceptance arcs by changing the conductance G_1. By setting the two conductances we may therefore synthesize all the reflection coefficients in the shaded area indicated in Fig. 4. The coverage area is then dependent on the diode spacing. The maximum amplitude of the reflection coefficient will depend on the phase asked for. For a particular phase setting α, the maximum possible amplitude can be written:

$$|\Gamma_d|_{\max} = \frac{\cos\frac{\theta}{2}}{-\cos\left(\frac{\theta}{2}+\alpha\right)+\sqrt{-\sin(\theta+\alpha)\sin\alpha}}. \tag{2}$$

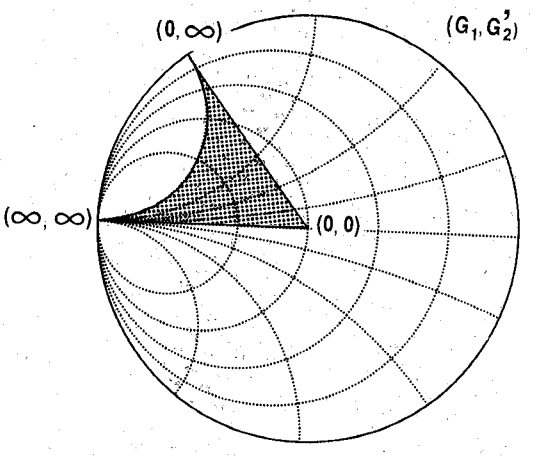

Fig. 4. Admittance coverage in the Smith chart for a pair of ideal diodes separated by a transmission line with length $\theta/2$.

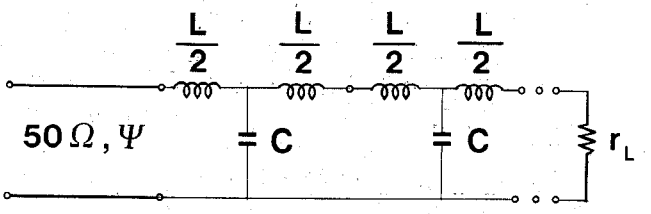

Fig. 5. Model of basic configuration.

The minimum value on the arc from $\pi-\theta$ to π is found when $\alpha = \pi - \theta/2$:

$$\min\{|\Gamma_d|_{\max}\} = \frac{\cos(\theta/2)}{1+\sin(\theta/2)}. \tag{3}$$

B. Artificial Transmission Line

It is essential to keep the diodes closely spaced to obtain a good coverage in the Smith chart. An accumulated loss from the capacitances of the p-i-n diodes is avoided by the use of an artificial transmission line.

A cascade of p-i-n diodes is mounted on a ground plane. The capacitance of the reversed p-i-n diodes and the interconnecting bonding wires then form an artificial transmission line (Fig. 5). To obtain a good simulation of a real transmission line, the phase of the subsections has to be small compared with the wavelength [8]. The artificial line impedance is given by

$$Z_0 = \sqrt{\frac{L}{C}}. \tag{4}$$

The inductance is dependent on the length of the bonding wire. The spacing of the diodes then determines the impedance level of the line. The transmission phase change of a section is

$$\angle S_{21} = \frac{\theta}{2} = -\frac{\pi}{2} + \tan^{-1}\left\{\frac{2rMN}{1-r^2M^2(N^2-1)}\right\} \tag{5}$$

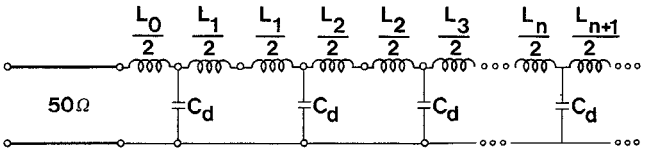

Fig. 6. Synthesis model.

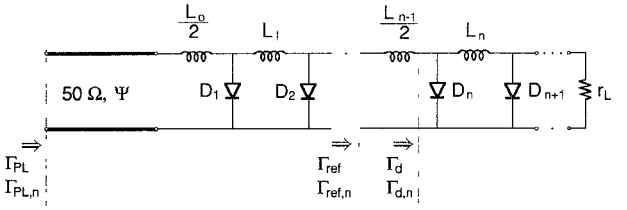

Fig. 7. Section definitions.

where

$$r = r_g = r_L$$

$$M = \frac{4}{\omega L}\,\frac{1}{4-\omega^2 LC}$$

$$N = \frac{2-\omega^2 LC}{2}.$$

III. Synthesis Procedure of Input Reflection Coefficient

In practice, the programmable load has a nonideal response. The algorithm which transforms a desired input reflection coefficient into bias currents for a chosen diode pair was made tolerant to these imperfections. This was done by abandoning the idea of a model with uniformly distributed, identical sections. Each section has its own individual model inductance (Fig. 6).

For the convenience of the reader, we specify the location of three different sections and the notations used for the corresponding reflection coefficients. They are at the diode, at the reference plane, and at the physical input of the programmable load (Fig. 7). The current driver setting procedure is divided in five steps.

A. Diode Pair Determination

The diode pair selection can be approximated from the measured values of the input reflection coefficients of fully forward biased diodes. The desired phase is to be located within the phase range of the selected diode pair. This selection is approximative because the diode is inside a unit element of the artificial transmission line.

Let us investigate the coverage area of the diode pair. The equivalent circuit and the Smith chart coverage are shown in Fig. 8. It can be seen from the coverage area plot that the phase coverage of the diode pair is amplitude dependent. If an inductance $L_{n-1}/2$ is included, we obtain the coverage area in the reference plane. In this case the phase coverage of the diode section is independent of the amplitude. We find that the distortion of Fig. 8 increases with decreasing amplitude. This is because the added inductance gives essentially a phase shift for high reflection coefficients, while both a phase and an amplitude shift are obtained for a smaller

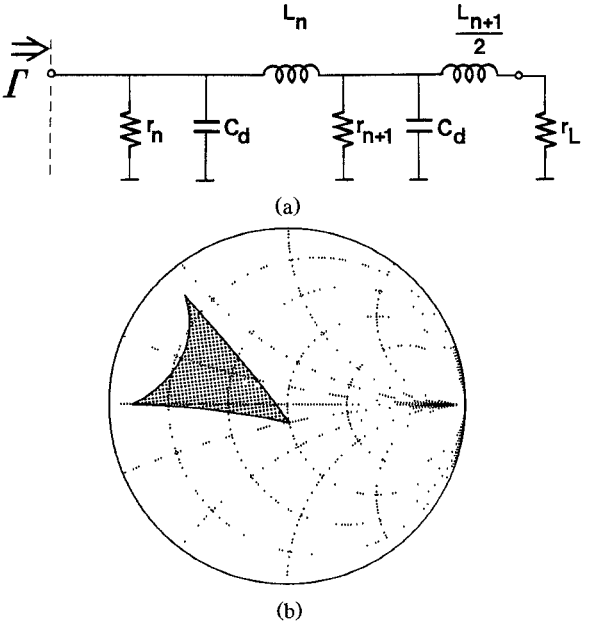

Fig. 8. Diode plane (a) Equivalent circuit (b) Coverage area.

reflection coefficient. The diode pair selection may therefore approximately be made from the measured values of the fully forward biased p-i-n diodes.

B. Transformation from Input to Reference Plane

A simple transmission line transformation is used to find the desired reflection coefficient in the reference plane from the desired reflection coefficient at the programmable load input:

$$\angle\Gamma_{\mathrm{ref,des}} = \angle\Gamma_{\mathrm{pl,des}} + 2\Psi \tag{6}$$

$$|\Gamma_{\mathrm{ref,des}}| = K_n|\Gamma_{\mathrm{pl,des}}|. \tag{7}$$

The phase of the input line and the artificial transmission line in front of the diode pair, 2Ψ, and the loss factor, K_n, are determined in the calibration part of this paper.

C. Diode Plane Reflection Coefficient

The reference plane reflection coefficient is now moved to the diode plane. The reflection coefficient is simply converted to corresponding input impedance and the inductance is subtracted. This is done in order to simplify the synthesis formulas.

D. Synthesis of Reflection Coefficient for a Diode Pair

The reflection coefficient asked for in the diode plane may be obtained by using derived synthesis formulas. These formulas are derived from a circuit consisting of two p-i-n diodes separated by an inductance, shown in Fig. 9. The input admittance for the circuit may be written as

$$Y_{\mathrm{in}} = Y_{d1} + \frac{Y_{d2} + Y_L}{1 + Z_b(Y_{d2} + Y_L)} \tag{8}$$

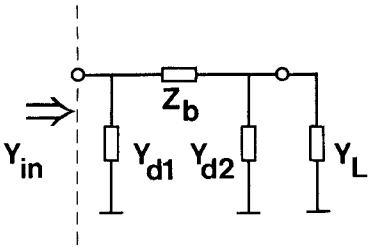

Fig. 9. Circuit used for synthesis of reflection coefficient.

where

$$Z_b = j\omega L_n$$
$$Y_{dk} = 1/r_{dk} + j\omega C_d, \qquad k = 1,2$$
$$Y_L = g_L + jb_L = 1\Big/\left(50 + \frac{j\omega L_{n+1}}{2}\right).$$

Solving for the two resistances, r_{d1} and r_{d2}, we get the formulas

$$g_{d2} = \frac{1}{r_{d2}} = -g_L + \left\{\frac{(1-\omega L_n b)}{\omega L_n} \cdot \left(b - \frac{\mathrm{Im}(Y_{\mathrm{in}}) - b_d}{1+\omega L_n(\mathrm{Im}(Y_{\mathrm{in}}) - b_d)}\right)\right\}^{1/2} \quad (9)$$

$$g_{d1} = \frac{1}{r_{d1}} = \mathrm{Re}(Y_{\mathrm{in}}) - \frac{g}{(1-\omega L_n b)^2 + (\omega L_n g)^2} \quad (10)$$

where

$$b = b_d + b_L$$
$$g = g_{d2} + g_L$$
$$Y_{\mathrm{in}} = \frac{1}{50}\frac{(1-\Gamma_{\mathrm{in}})}{(1+\Gamma_{\mathrm{in}})}.$$

E. Resistance to Bias Current Conversion

The final step is to convert the synthesized resistances to corresponding p-i-n diode bias currents.

IV. Parameter Determination

The p-i-n diode parameters are determined separately. Other parameters are determined by calibration measurements at the input port.

A. p-i-n Diode Characterization

An MA47403 p-i-n diode was mounted in a fixture. The input reflection coefficient was measured in the frequency range 4–8 GHz for several diode currents. The fixture and the diode were modeled using TOUCHSTONE. The 0.00, 0.023, 0.811, and 3.207 mA measurements were simultaneously fitted to four different models. All the model parameters, with the exception of the diode resistance r_d, were shared by all four models. All well-defined parameters of the fixture, such as transmission line lengths and impedances, were fixed during the optimization. The resulting diode parameters were

$$C_d = 0.186 \text{ pF} \qquad L_d = 28 \text{ pH}.$$

With all other parameters fixed, r_d was determined for all the diode currents. The parameters of the $I_d - r_d$ relationship [9] were then optimized to fit these data.

The result of the optimization was

$$r_d(I[\mathrm{mA}]) = a + b\cdot I^{-c} = 1.585 + 8.132\cdot I^{-0.864}. \quad (11)$$

The maximum error in r_d corresponds to a maximum error in the measured reflection coefficient of 0.025.

B. Determination of Unknown Parameters from External Measurements

A calibration of the programmable load is made in order to determine unknown parameters. All calibration measurements are made at the input port. The bonding wire inductances could have been measured and modeled by themselves. It is, however, desirable to allow for imperfections in the practical design. The inductances will therefore not be the actual bonding wire inductances, but will also include different parasitic components which distort the response of the programmable load. The inductances will mainly influence the phase response.

The amplitude response has been corrected for two different effects. The first is the loss along the line. These corrections are accurate for higher reflection coefficients. For lower reflection coefficients, the parasitic components have been corrected for by adjusting the b parameter of the current-to-resistance relationship. In the calibration procedure the following parameters are therefore determined:

- inductance L_n adjusts the phase response;
- loss factor K_n adjusts the amplitude response for high reflection coefficient;
- parameter b_n adjusts the magnitude response for low reflection coefficients.

1) Calibration Measurements: The input reflection coefficients of the programmable load are measured when the diodes are fully, $\Gamma^F_{\mathrm{pl},n}$, or partially, $\Gamma^P_{\mathrm{pl},n}$, biased one by one along the diode line.

The chosen magnitude of $\Gamma^P_{\mathrm{pl},n}$ determines the magnitude level besides the maximum magnitude for which the synthesis algorithm will be most accurate. This level was chosen to about 0.2.

2) Inductance Calculation: The inductance is determined by comparing the measured and the calculated phase coverage. As a diode that is fully on produces a reflection phase of approximately 180°, it is possible to determine the phase coverage from

$$\theta_{n,\,\mathrm{measured}} = \angle\Gamma^F_{\mathrm{pl},n} - \angle\Gamma^F_{\mathrm{pl},n-1}. \quad (12)$$

In Fig. 10 only L_n and L_{n-1} are unknown. As the diode resistance is very small, the effect of the inductance, L_n, is insignificant. The phase shift of a section is then

$$\theta_{n,\,\mathrm{calculated}} = \pi - \angle\Gamma^F_{d,n}. \quad (13)$$

The inductance L_{n-1} is determined by a Fibonacci search routine.

3) Determination of ψ and K_n: The phase of the input line and the artificial transmission line in front of the diode pair is obtained from

$$2\Psi = \angle\Gamma^F_{\mathrm{ref},n} - \angle\Gamma^F_{\mathrm{pl},n}. \quad (14)$$

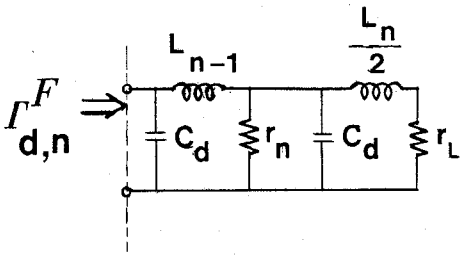

Fig. 10. Reflection phase consideration using a fully forward biased diode.

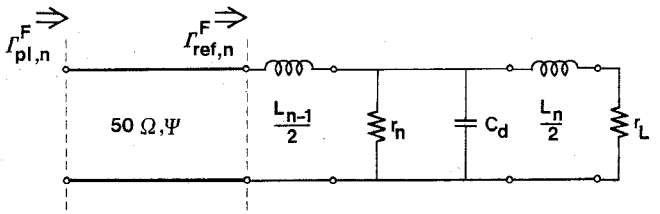

Fig. 11. Reflection phase considerations using an active diode pair.

The input reflection coefficient, $\Gamma^F_{\mathrm{pl},n}$, is measured while the reference plane reflection coefficient, $\Gamma^F_{\mathrm{ref},n}$, is calculated from the known parameters of Fig. 11. The loss factor, K_n, is determined in the same way from measured and calculated values:

$$K_n = \frac{|\Gamma^F_{\mathrm{ref},n}|}{|\Gamma^F_{\mathrm{pl},n}|}. \tag{15}$$

4) Diode b Parameter Calculation: From the known diode current and the known diode parameters a and c, the b parameter is directly related to the diode resistance r_d. The diode resistance is determined from the measured input reflection coefficient of the programmable load for a partially on p-i-n diode. The adjusted value of r_d will now give the same input reflection coefficients as the actual r_d gives in an ideal structure. The quantity r_d is calculated by first moving the measured reflection coefficient from the input of the load to the reference plane:

$$\angle \Gamma^P_{\mathrm{ref},n} = \angle \Gamma^P_{\mathrm{pl},n} + 2\Psi \tag{16}$$

$$|\Gamma^P_{\mathrm{ref},n}| = K_n |\Gamma^P_{\mathrm{pl},n}|. \tag{17}$$

The diode resistance, r_d, is then de-embedded.

V. Design

A. Number of Diodes

To obtain a full phase coverage of the programmable load, the line must have an electrical length of 180° at the lowest frequency, 4 GHz. By using the commercial CAD program TOUCHSTONE 15 diodes were found to provide a full phase coverage. At 8 GHz only half of the line is used. The physical length of the line is close to 12 mm. With ideal components, the amplitude of the reflection coefficient for which all phase settings can be used are 0.81 at 4 GHz, 0.73 at 6 GHz and 0.65 at 8 GHz, all according to (3).

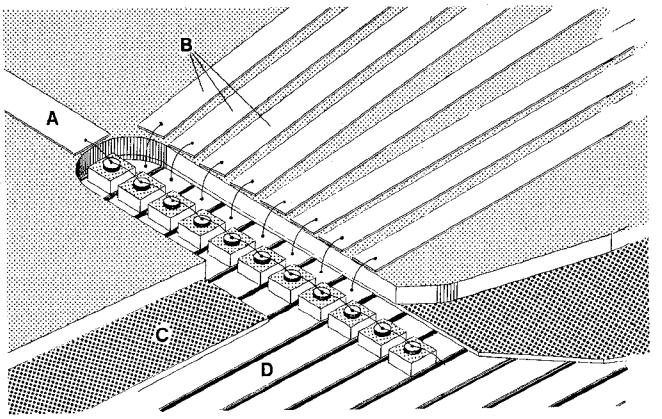

Fig. 12. Programmable load realization: (*A*) 50 Ω microstrip RF-feed; (*B*) dc supply lines; (*C*) combined microstrip and stripline RF ground plane; (*D*) virtual RF ground plane for the p-i-n diodes.

B. Diode Biasing

The narrow diode spacing makes it difficult to design a biasing network for each diode. There is no space for dc-isolating capacitors if a good coverage is to be obtained. To solve this design problem a novel biasing technique is used. The diode is placed directly on two open-ended quarter-wavelength stripline stubs. A virtual RF ground at the diode is in this way provided by the stubs. The dc bias can now individually be fed to each diode at the virtual RF ground without affecting the RF performance. A common bias terminal is provided via the bonding wires of the diode line. The common bias can then be supplied using a conventional bias T at the output of the programmable load. A microstrip substrate is placed on top of the stripline structure (Fig. 12). This substrate is used for the RF supply and dc supply to the diode line. A groove is cut in the stripline structure to provide access to the diode line. Microstrip lines connect the diode line and the coaxial connectors. A continuous bonding wire connects all the diodes. There are 15 dc supply lines from a 16 DIL connector to the edge of the groove. Each of these lines is connected to a diode virtual RF ground.

C. Construction

To make a wide-band virtual ground, the $\lambda/4$ stubs should have the lowest possible impedance. As the need for a small diode spacing limited the width of the stubs to 0.7 mm, a thin substrate had to be used. A Di-clad 522 laminate with a thickness of 0.097 mm was used. This width and thickness result in a line impedance of 12 Ω. For the stripline substrate, a 0.38-mm-thick Di-clad 522 was chosen as a compromise in considering physical rigidity, microstrip–coax match, and bonding distance between the microstrip lines and the diodes.

VI. Simulation of the Programmable Load

The programmable load was modeled to gain a better understanding of the structure and to check the results of the diode characterization. The programmable load model is divided into three blocks: the two RF feeds separated by the artificial transmission line. The models of the RF feeds were: coaxial line–transition–microstrip line. The transitions were modeled by π networks: capacitor to ground–series induc-

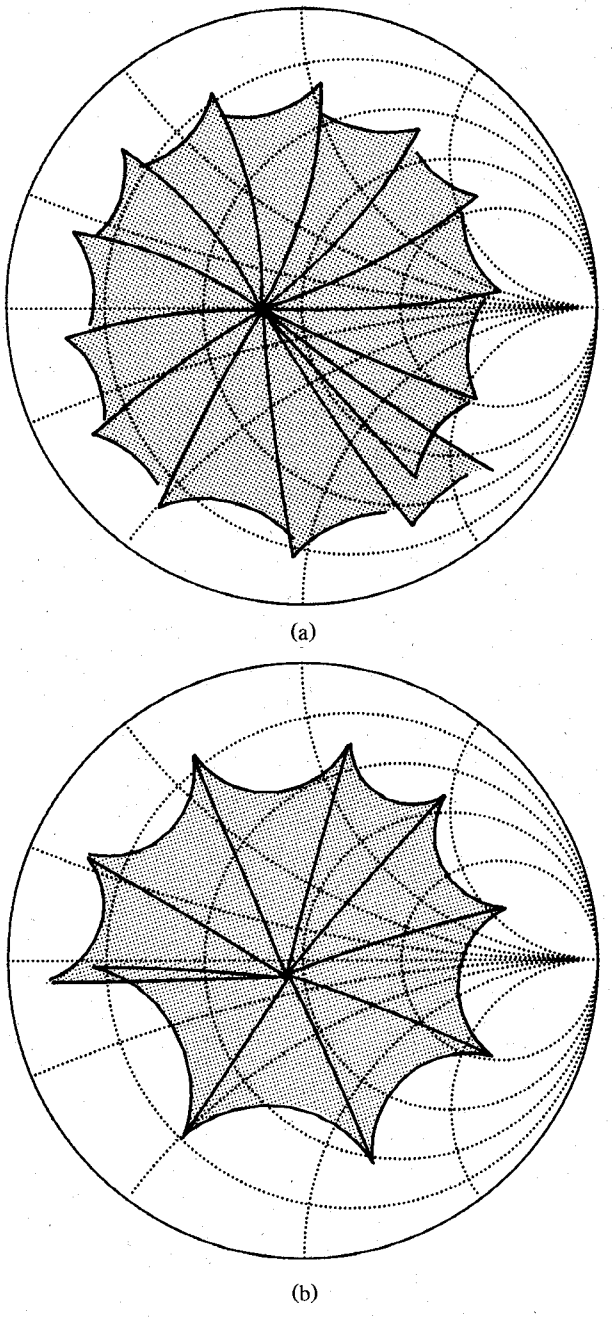

Fig. 13. Measured coverage area of the programmable load: (a) 4 GHz, (b) 6 GHz.

tance–capacitor to ground. The artificial transmission line was modeled by 15 cascaded diode modules. The virtual RF ground of the module was modeled by two stripline stubs including open end effects. The characteristic impedance of the diode line was obtained from the time-domain measurement. The p-i-n diode capacitance and the average bond wire inductance were determined by comparing simulated and measured phase coverage:

$$L = 0.49 \text{ nH} \qquad C_d = 0.18 \text{ pF}.$$

The deviation from the capacitance value obtained in the p-i-n diode characterization is explained by measurement uncertainties.

Good agreement between models and measured data in the time and frequency domains was obtained for the fixture

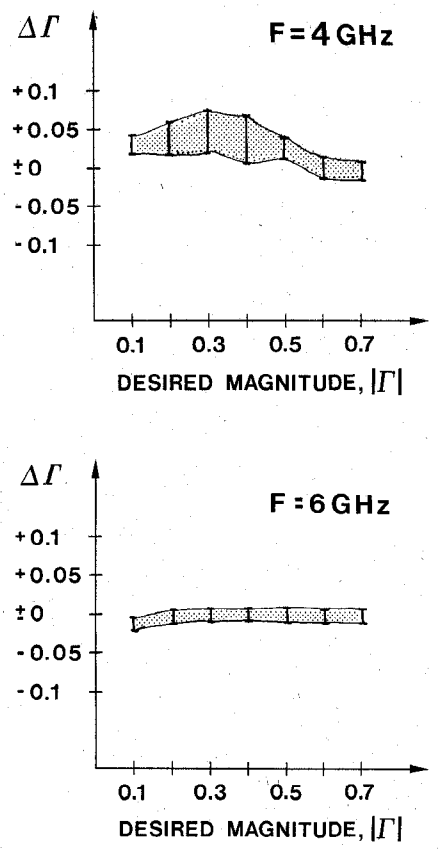

Fig. 14. Measured magnitude error versus desired magnitude. Shaded areas show the standard deviation.

(Section IV) and for the programmable load. TOUCHSTONE was used for the frequency-domain modeling and SPICE for the time-domain modeling.

VII. Measurements

The coverage area and errors in synthesized reflection coefficients for the programmable load have been measured.

A. Measurement of Coverage Area

The load can be continuously set to any impedance within its coverage area. The coverage areas for 4 and 6 GHz are shown in Fig. 13.

B. Measured Results from Desired Magnitude and Phase Settings

The accuracy of the synthesis procedure has been measured. In Fig. 14, we show the magnitude error ($\Delta\Gamma$) versus desired magnitude ($|\Gamma|$) at the frequencies 4 and 6 GHz. In Fig. 15, we show the resulting phase error versus desired magnitude at the same frequencies. For high-accuracy applications, the good reproducibility of the programmable load can be used by measuring the reflection coefficient before or after the DUT measurement.

VIII. Noise of Programmable Load

The programmable load has been used in a computer-controlled noise parameter measurement system developed by the authors [10]. This system does not require the pro-

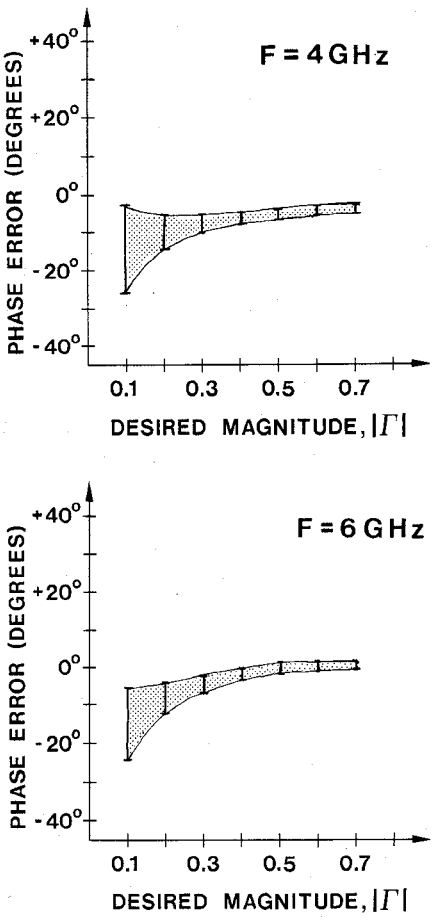

Fig. 15. Measured phase error versus desired magnitude. Shaded areas show the standard deviation.

grammable load to be noiseless. The noise figure is measured and taken into account when the noise figure of the actual DUT is calculated. However, the programmable load has been found to add very little noise and can be treated as a passive device. This may be partly explained by the fact that only two diodes are biased at the time and partly by the fact that when high currents go through the diodes the noise power is short-circuited.

Two types of measurements have been performed to investigate the possibility of using the programmable load as a passive device in our noise parameter measurement system:

1) Noise power output from programmable load.
2) Programmable load has been used as a passive device in verifying measurements of the complete noise parameter measurement system [10].

A. Output Noise Power of Programmable Load

The noise figure meter HP 8970A was used in the power density mode to measure the output power of the programmable load. The system was first calibrated by connecting the noise source, 346B, at the input of the circulator. The calibrated data were used to compensate the readout of the noise figure meter to give the absolute input power density related to kT_0 (available power of resistor at 290 K).

The noise output power has been measured for different settings of the programmable load. The readout of the noise figure meter for these measurements could not be distinguished from the measurement of a 50 Ω termination.

When the PL is matched, all of the output power is engendered within the load. On the other hand, if the load is mismatched the circulator termination adds to the output power. This does not present a problem for the measurement as it represents the actual use of the load.

B. System Measurement

The programmable load has been used in the complete system [10]. The noise factor and the available gain of the programmable load assembly (PL + Switch + Coupler + bias T) has been measured taking the second stage and mismatch effects into account. The product $F \cdot G_a$ was close to unity for these measurements. This confirms that the programmable load can be treated as a passive device.

IX. Conclusions

A new computer-controlled programmable load has been presented. The load consists of a cascade of p-i-n diodes bonded to each other. The interconnecting bonding wires together with the capacitance of the reversed biased p-i-n diode form an artificial transmission line. A complete phase coverage in the Smith chart is obtained by forward-biasing any diode pair, using only two current generators and two multiplexers. The load may be set to any reflection coefficient within its coverage area by using synthesis formulas for the determination of the current driver settings. Measurements verify the principle and show good agreement with simulations. The load has been developed for noise parameter determination but is also believed to be of interest in other areas.

Acknowledgment

The authors would like to thank A. Olausson for the design and construction of the microprocessor-controlled bias circuits.

References

[1] IRE Subcommittee on Noise, "IRE standards on methods of measuring noise in linear twoports, 1959," *Proc. IRE*, vol. 48, pp. 60–68, Jan. 1960.
[2] R. Q. Lane, "The determination of device noise parameters," *Proc. IEEE*, vol. 57, pp. 1461–1462, Aug. 1969.
[3] N. J. Kuhn, "Curing a subtle but significant cause of noise figure error," *Microwave J.*, pp. 85–98, June 1984.
[4] R. D. Pollard, M. Pierpoint, M. Maury, S. L. March, and G. R. Simpson, "Programmable tuner system characterizes gain and noise," *Microwave & RF*, pp. 265–269, May 1987.
[5] B. W. Leake, "A programmable load for power and noise characterization," in *IEEE MTT-S Symp. Int. Microwave Dig.*, 1982, pp. 348–350.
[6] J. P. Starski and B. Albinsson, "An absorptive attenuator with optimized phase response," presented at 14th European Microwave Conf., Liege, Belgium, Sept. 10–13, 1984.
[7] K. Wilson, J. M. C. Nichols, G. McDermott, and J. W. Burns, "A novel MMIC X-band phase shifter," *IEEE Trans. Microwave Theory Tech.*, vol. MTT-33, pp. 1572–1578, Dec. 1985.
[8] K. B. Niclas, W. T. Wilser, T. R. Kritzer, and R. R. Pereira, "On theory and performance of solid-state microwave distributed amplifiers," *IEEE Trans. Microwave Theory Tech.*, vol. MTT-31, pp. 447–456, June 1983.
[9] R. V. Garver, *Microwave diode control devices*. Norwood, MA: Artech, 1976.
[10] B. Albinsson, H. Guo, M. Schöön, and H-O. Vickes, "A computer controlled noise parameter measurement system," Divi-

sion of Network Theory, Tech. Rep. No. 9002, Chalmers University of Technology, Gothenburg, Sweden, Aug. 1990.

Björn M. Albinsson (S'82) was born in Visby, Sweden, in 1958. He received the M.Sc. (1983), Tekn. Licentiat (1987), and Ph.D. (1990) degrees from the Electrical Engineering Department of Chalmers University of Technology, Gothenburg, Sweden.

He is presently with the Division of Applied Electron Physics at Chalmers University of Technology. His current research interests include LNA design, CAD techniques, and noise parameter determination.

Henglo Guo was born in Shanghai, China, on March 3, 1944. He received the diploma in electronic engineering from the Harbin Institute of Engineering in 1967 and the M.Eng. degree in electronic communication from the Post and Telecommunication Science Research Academy, Shanghai, China, in 1981.

From 1982 to 1984, he worked as a research engineer at the Nanjing Electronic Devices Research Institute, Nanjing, China. During the years 1984 to 1986, he was a guest researcher at the Institute of Microwave Technology in Stockholm, Sweden. From 1986 to 1989, he was a guest researcher in the Department of Radio and Space Science, Chalmers University of Technology, Gothenburg, Sweden. His activities are mainly in the area of microwave circuits and involve computer-aided design, device characterization, low-noise amplifiers, and measurement techniques.

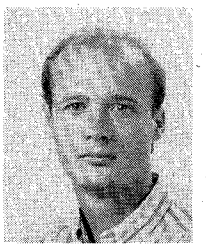

Martin Schöön (S'90) was born in Gothenburg, Sweden, in 1960. He received the M.Sc. degree in electrical engineering from Chalmers University of Technology, Gothenburg, Sweden, in 1984. He is currently studying for the Ph.D. degree in the Division of Network Theory, Chalmers University of Technology. His current research interests include the measurement and characterization of active microwave devices.

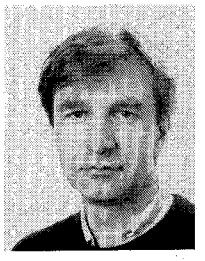

Hans-Olof Vickes (S'88) was born in Malung, in the province of Dalecarlia, Sweden, in 1954. He received the degrees of Civilingenjör (M.Sc.), Tekn. Licentiat, and Doctor of Philosophy in 1982, 1988, and 1990 respectively, from the Electrical Engineering Department of Chalmers University of Technology, Gothenburg, Sweden. His doctoral thesis dealt with microwave and millimeter-wave FET's and noise parameter measurements.

In October 1990 he joined the Aerospace Division at Ericsson Radar Electronics, Mölndal, Sweden.